# Perfect and Near-Perfect Adaptation in a Model of Bacterial Chemotaxis

Bernardo A. Mello*[†] and Yuhai Tu*

*IBM T. J. Watson Research Center, Yorktown Heights, New York, USA; and [†]Physics Department,
Catholic University of Brasilia, Brasilia, DF, Brazil

ABSTRACT   The signaling apparatus mediating bacterial chemotaxis can adapt to a wide range of persistent external stimuli. In many cases, the bacterial activity returns to its prestimulus level exactly, and this perfect adaptability is robust against variations in various chemotaxis protein concentrations. We model the bacterial chemotaxis signaling pathway, from ligand binding to CheY phosphorylation. By solving the steady-state equations of the model analytically, we derive a full set of conditions for the system to achieve perfect adaptation. The conditions related to the phosphorylation part of the pathway are discovered for the first time, while other conditions are generalizations of the ones found in previous works. Sensitivity of the perfect adaptation is evaluated by perturbing these conditions. We find that, even in the absence of some of the perfect adaptation conditions, adaptation can be achieved with near-perfect precision as a result of the separation of scales in both chemotaxis protein concentrations and reaction rates, or specific properties of the receptor distribution in different methylation states. Since near-perfect adaptation can be found in much larger regions of the parameter space than that defined by the perfect adaptation conditions, their existence is essential to understand robustness in bacterial chemotaxis.

## INTRODUCTION

The motion of coliform bacteria (such as *Escherichia coli*) is driven by rotation of several flagella attached to the cell body. When the flagella rotate counterclockwise (CCW), the flagella form a bundle that pushes the bacterium in a smooth motion (runs) with a high degree of directionality. On the other hand, when the flagella rotate clockwise (CW), the flagella bundle flies apart and the bacterium tumbles, randomizing the direction of the subsequent run. The frequency with which the tumbling motion occurs decreases with increasing concentration of attractant (or decreasing concentration of repellent). As the result, the bacterium performs a biased random walk toward higher concentration of attractant. This mechanism gives the bacterium its ability to follow the gradient of chemical concentration, i.e., chemotaxis.

From the sensing of external stimulus to the activation of motor regulator protein, a series of chemical reactions are involved in relaying and regulating the signal. (For recent reviews on the bacterial chemotaxis signaling pathway, see Falke et al., 1997; Bren and Eisenbach, 2000; and Bourret and Stock, 2002.) The major players in the chemotaxis signal transduction pathway are the transmembrane chemotaxis receptors and six cytosolic proteins: CheA, CheB, CheR, CheW, CheY, and CheZ. The receptor forms a complex with the histidine kinase CheA through the adaptor protein CheW. The receptor has a ligand-binding domain located at the periplasm to sense the external signal, such as the concentration of attractant (or repellent). The activity of CheA is affected by the properties of the receptor; for example,

whether the receptor is ligand-bound or not. When chemoattractant binds to receptor, CheA activity is suppressed. The histidine kinase CheA, once activated, acquires a phosphate group through autophosphorylation, and subsequently transfers the phosphate group to the response regulator protein CheY or the demethylation enzyme CheB. The phosphorylated CheY (CheY-P) then interacts with the motor and increases the motor's CW rotation bias. This is the linear signal transfer part of the bacterial chemotaxis pathway. Like many other biological sensory systems, the bacterial chemotaxis pathway also has the ability to adapt to persistent external stimulus. The adaptation in bacterial chemotaxis is facilitated by the methylation and demethylation of the receptor, which serves as the feedback control of the system. The methylation and demethylation processes are catalyzed by CheR and CheB-P, respectively, and are slow in comparison with the other reactions.

Because of the excellent understanding of each individual reaction of the pathway, mathematical modeling of bacterial chemotaxis signal transduction has been very fruitful (Bray et al., 1993; Hauri and Ross, 1995; Barkai and Leibler, 1997; Spiro et al., 1997; Morton-Firth and Bray, 1998; Morton-Firth et al., 1999; Yi et al., 2000). Besides being useful in understanding specific aspects of chemotaxis experiments, modeling is essential in gaining insight about general properties of biochemical networks. One important general problem is to understand the functional stability of biochemical networks under changes of various pathway parameters, such as concentrations of enzymes and reaction rates. Parameter fluctuations are inherent for biological systems in the real world, so robustness, i.e., the insensitivity of important system properties with respect to parameter variation and fluctuation of protein concentrations, is crucial for the proper functioning of the biological systems.

Experimentally, it was observed that after initial response to some external stimulus, such as sudden changes of

aspartate concentrations, the bacteria tumbling frequency often reverts to its original value with high accuracy, independent of the strength of the external stimulus (Berg and Brown, 1972). This accurate adaptation is generally believed to contribute to the high sensitivity of bacterial chemotaxis to a wide range of external stimulus (five orders of magnitude). In a recent work, Barkai and Leibler (1997) investigated the robustness of perfect adaptation in bacterial chemotaxis; they used a two-state (active or inactive) model (Asakura and Honda, 1984) for the receptor complex in explaining the phenomena. In their model, they assumed that CheB only demethylates active receptors, whereas CheR methylates all receptors indiscriminately. They showed, by extensive simulation of the two-state model, that as long as the above conditions are satisfied, adaptation is achieved with high precision, independent of specific values of the rate constants or enzyme concentrations. In a subsequent study, Alon and co-workers (Alon et al., 1999) provided experimental evidence for the robustness of the perfect adaptation over large variations in chemotactic protein concentrations.

The Barkai-Leibler (BL) model clearly captured one of the essential ingredients for perfect adaptation in bacterial chemotaxis. Recently, Yi and colleagues (Yi et al., 2000) further studied the Barkai-Leibler model analytically, and summarized all the conditions for perfect adaptation within the BL model beyond those identified in the original article. However, the BL model is a simplified description of the real chemotaxis pathway. For example, the BL model neglects the phosphorylation part of the pathway altogether and assumes the saturation of methylation enzyme CheR, which is questionable (Morton-Firth et al., 1999).

In this work, we study a more complete model of the chemotaxis signal transduction pathway, similar to the deterministic version of the model proposed by Morton-Firth and co-workers (Morton-Firth et al., 1999), where both the methylation and phosphorylation processes are taken into account. Our goals are to understand whether (mathematically) perfect adaptation—defined as when steady-state CheY-P concentration is independent of ligand concentration—can be achieved for the full model, and to identify the conditions for such perfect adaptation. The sensitivity of the perfect adaptability, or robustness, is then studied by perturbing these conditions. Such study can help us understand adaptation in real biological systems where not all the perfect adaptation conditions are satisfied. It can also provide possible explanations for cases where perfect adaptation is not achieved, e.g., for serine response (Berg and Brown, 1972).

## MODEL

For the purpose of this study, we consider only those receptors that form complex with CheW and CheA. We label the receptor complex by $T_{n\lambda}$, where $n (\in [0,4])$ is the number of methyl groups added to the receptor and $\lambda (=o, v)$ rep-

resents the ligand occupied ($o$) and vacant ($v$) state of the receptor. Superscripts are also used to describe whether the receptor complex is phosphorylated ($P$) or unphosphorylated ($U$), bound to CheR/CheB-P, or free ($F$). Superscript ($T$) is used to label total concentrations of different proteins. The superscripts are not mutually exclusive, e.g., $[B^{PF}]$ is the concentration of phosphorylated free (not bound to receptor) CheB. In Table 1, some of the chemical species of the chemotaxis pathway are shown, where the values of the total concentrations are taken from Morton-Firth et al. (1999), except for the total CheR concentration, which we have reduced slightly to have the same average methylation level as reported in Morton-Firth et al. (1999), where receptors other than Tar were included in the simulation.

The bacterial chemotaxis pathway can be divided into three processes: receptor ligand binding, receptor methylation/demethylation, and phosphorylation of CheA, CheB, and CheY. The reactions involved in each of the three processes are listed in Table 2. Since the ligand-binding process is much faster than the other two, the ligand-binding reaction can be considered to be always in quasi-equilibrium. The receptor's ligand-binding status directly affects both the CheA autophosphorylation rate and the receptor methylation/demethylation rates. The CheA autophosphorylation rate is also affected by the methylation state of the receptor. Finally, since only the phosphorylated CheB can efficiently demethylate the receptor, the methylation process is also affected by the phosphorylation process.

Some conformational change of the receptor complex is probably responsible for the signaling from binding of ligand to methylation and phosphorylation of the receptor complex (Bren and Eisenbach, 2000; Falke et al., 1997; Liu et al., 1997). The two-state model proposes that the receptor complex has two states, active and inactive, with only the active state capable of autophosphorylation. For a receptor with $n$-methyl groups and a ligand occupancy status described by

**TABLE 1  Chemical species and subspecies: total concentrations are taken from Morton-Firth et al. (1999)**

| Species | Description | Concentration |
|---------|-------------|---------------|
| $[T^T]$ | Total taxis aspartate receptor (Tar) | 2.5 $\mu$M |
| $[T_{n\lambda}]$ | Receptor with $n$-methyl groups, ligand binding site occupied ($\lambda = o$) or vacant ($\lambda = v$) | |
| $[T^F]$ | Free (CheR and CheB unbound) receptor | |
| $[T^P]$ | Phosphorylated receptor | |
| $[T^U]$ | Unphosphorylated receptor | |
| $[R^T]$ | CheR | 0.176 $\mu$M |
| $[R^F]$ | Free (not bound to $T$) CheR | |
| $[B^T]$ | CheB | 2.27 $\mu$M |
| $[B^F]$ | Free (not bound to $T$) CheB | |
| $[B^P]$ | Phosphorylated CheB | |
| $[B^{PF}]$ | Free phosphorylated CheB | |
| $[Y^T]$ | CheY | 18 $\mu$M |
| $[Y^P]$ | Phosphorylated CheY | |

**TABLE 2  Chemotaxis signal transduction reactions**

| Ligand binding | $T_{nv} + L \leftrightarrow T_n L (\equiv T_{no})$ | |
|---|---|---|
| Methylation | $T_n + R^F \leftrightarrow T_n R$ | $T_n R \rightarrow T_{n+1} + R^F$ |
| | $T_n + B^{PF} \leftrightarrow T_n B^P$ | $T_n B^P \rightarrow T_{n-1} + B^{PF}$ |
| Phosphorylation | $T_n^U \rightarrow T_n^P$ | |
| | $T_n^P + Y^U \rightarrow T_n^U + Y^P$ | $Y^P \rightarrow Y^U$ |
| | $T_n^P + B^{UF} \rightarrow T_n^U + B^{PF}$ | $B^{PF} \rightarrow B^{UF}$ |

$\lambda$ (vacant, $v$, or occupied, $o$), the probability of being active is denoted by $P_{n\lambda}$. However, there has been no direct experimental evidence in support of the two-state model (Yi et al., 2000). More generally, $0 \leq P_{n\lambda} \leq 1$ can be simply understood as the relative receptor activity for receptor $T_{n\lambda}$, and the CheA autophosphorylation rate is proportional to $P_{n\lambda}$:

$$k_{n\lambda}^P = k^P P_{n\lambda}, \tag{1}$$

where $k^P$ is a constant independent of $n$ and $\lambda$.

In the following, we write down all the equations for the reactions listed in Table 1. The ligand binding reaction is given by:

$$T_{nv} + Ligand \underset{k_{b,n}}{\overset{k_{f,n}}{\rightleftarrows}} T_{no}. \tag{2}$$
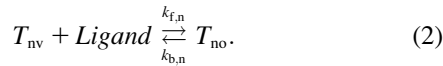
Since the timescale for ligand binding is much shorter than the other reactions, the ligand binding reaction can be assumed to be in quasi-equilibrium and the two populations for each methylation level can then be written as:

$$[T_{nv}] = (1 - L_n)[T_n], \tag{3}$$

$$[T_{no}] = L_n[T_n], \tag{4}$$

where $L_n \equiv [L]/([L] + K_{d,n})$, is the receptor occupancy rate, $[L]$ is the ligand concentration, and $[T_n] = [T_{no}] + [T_{nv}]$ is the total receptor population in methylation level $n$. The ligand receptor dissociation constant $K_{d,n}$ ($\equiv k_{b,n}/k_{f,n}$) probably depends on the methylation level of the receptor $n$ (Dunten and Koshland, Jr., 1991; Borkovich et al., 1992; Bornhorst and Falke, 2001; Sourjik and Berg, 2002); however, it will become clear later that this does not affect the perfect adaptation conditions.

The methylation/demethylation reactions can be written as:

$$T_n + E \rightleftharpoons T_n E \longrightarrow T_{n\pm 1} + E, \tag{5}$$
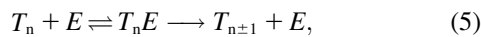
where the enzyme $E$ is either $R$ (CheR) or $B$ (CheB-P). Here we assume the methylation/demethylation process at the four methylation sites follows a preferred sequence, and therefore the existence of only five methylation states is described by $n \in [0,4]$. Though this assumption is still an open question, it is supported by some experiments (Shapiro and Koshland, Jr., 1994; Shapiro et al., 1995). The network of methylation/demethylation reactions are illustrated in Fig. 1.

If we assume the above reactions follow Michaelis-Menten kinetics and the dissociation rates for the bound state are independent of $\lambda$, i.e., whether the receptor is ligand-bound or not, the bound state concentration can be written as:
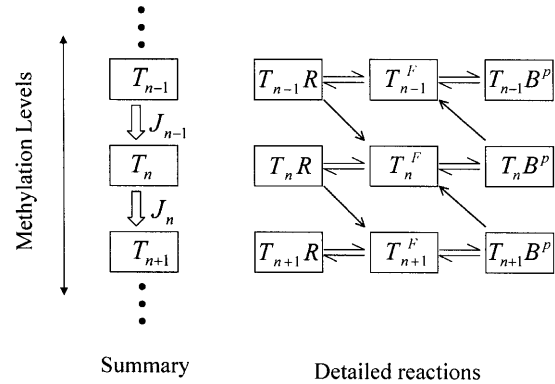


FIGURE 1  Illustration of the methylation and demethylation reaction network; $n$ is the methylation level of the receptor.

$$[T_n E] = \frac{[T_n^F][E^F]}{K_n^E}, \tag{6}$$

where $K_n^E = [(1 - L_n)K_{nv}^{E-1} + L_n K_{no}^{E-1}]^{-1}$ is the Michaelis constant of the combined (vacant and ligand-bound) receptor state and the superscript $F$ denotes the free enzyme and the free substrate (receptor) concentrations.

Since the receptors and the enzymes can exist either in their free form or bound to each other, the total concentrations of enzymes, and the concentration of receptors with $n$-methylated sites, are given by the following equations:

$$[R^T] = [R^F]\left(1 + \sum_{n=0}^{4} \frac{[T_n^F]}{K_n^R}\right), \tag{7}$$

$$[B^P] = [B^{PF}]\left(1 + \sum_{n=0}^{4} \frac{[T_n^F]}{K_n^B}\right), \tag{8}$$

$$[T_n] = \left(1 + \frac{[R^F]}{K_n^R} + \frac{[B^{PF}]}{K_n^B}\right)[T_n^F], \tag{9}$$

where the $[R^T]$, $[B^P]$, and $[T_n]$ are the concentrations of CheR, phosphorylated CheB, and receptors with $n$-methyl groups, respectively.

The kinetic equation for the receptor concentrations $[T_n]$ at each methylation level can be written as:

$$\frac{d[T_n]}{dt} = J_{n-1} - J_n, \tag{10}$$

where $J_n$ is the net flux from methylation level $n$ to level ($n + 1$), which is just the difference of methylation and demethylation rates between these two states. Using the bound state concentration given in Eq. 6, $J_n$ can be written as:
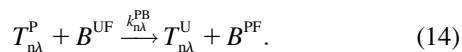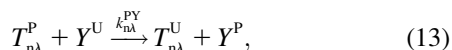
$$J_n = k_n^R \frac{[R^F][T_n^F]}{K_n^R} - k_{n+1}^B \frac{[B^{PF}][T_{n+1}^F]}{K_{n+1}^B}, \quad (0 \leq n \leq 3), \tag{11}$$

where $k_n^R$ and $k_n^B$ are the catalytic constants for the methylation and demethylation reaction respectively, which are assumed to be independent of $\lambda$, the ligand-binding status of the receptor. The boundary conditions for the methylation flux are: $J_{-1} = J_4 = 0$.

The autophosphorylation of CheA reaction is given by:

$$T_{n\lambda}^{U} \xrightarrow{k_{n\lambda}^{P}} T_{n\lambda}^{P}, \tag{12}$$

the phosphate group is subsequently transferred from CheA-P to CheB and CheY:

$$T_{n\lambda}^{P} + Y^{U} \xrightarrow{k_{n\lambda}^{PY}} T_{n\lambda}^{U} + Y^{P}, \tag{13}$$

$$T_{n\lambda}^{P} + B^{UF} \xrightarrow{k_{n\lambda}^{PB}} T_{n\lambda}^{U} + B^{PF}. \tag{14}$$

While CheB-P dephosphorylates spontaneously, the CheY-P hydrolysis is enhanced by the phosphatase CheZ, an effect that is included in the high hydrolysis rate $k^{HY}$ for CheY-P (Lukat et al., 1991):

$$Y^{P} \xrightarrow{k^{HY}} Y, \tag{15}$$

$$B^{PF} \xrightarrow{k^{HB}} B^{UF}. \tag{16}$$

The kinetic equations for these reactions are:

$$\frac{d[Y^{P}]}{dt} = \sum_{n=0}^{4} k_{n}^{PY}[T_{n}^{P}][Y^{U}] - k^{HY}[Y^{P}], \tag{17}$$

$$\frac{d[B^{PF}]}{dt} = \sum_{n=0}^{4} k_{n}^{PB}[T_{n}^{P}][B^{UF}] - k^{HB}[B^{PF}], \tag{18}$$

$$\frac{d[T_{n}^{P}]}{dt} = k_{n}^{P}[T_{n}^{U}] - k_{n}^{PY}[T_{n}^{P}][Y^{U}] - k_{n}^{PB}[T_{n}^{P}][B^{UF}] + J_{n-1}^{P} - J_{n}^{P}, \tag{19}$$

where $[Y^{U}] = [Y^{T}] - [Y^{P}]$, $[B^{UF}] = [B^{F}] - [B^{PF}]$, and $[T_{n}^{U}] = [T_{n}] - [T_{n}^{P}]$. $J_{n}^{P}$ is the net phosphorylated receptor flux between methylation level $n$ and $(n + 1)$, given similarly as for $J_{n}$ in Eq. 11 with the free receptor concentration $[T_{n}^{F}]$ replaced by the phosphorylated free receptor concentration $[T_{n}^{FP}]$. In all the above equations, the dependence on $\lambda$ is omitted, so the autophosphorylation rate and the phosphate transfer rates should all be considered as the rate for the combined receptor state (ligand occupied and unoccupied):

$$k_{n}^{P} = L_{n}k_{no}^{P} + (1 - L_{n})k_{nv}^{P}, \quad k_{n}^{PY} = L_{n}k_{no}^{PY} + (1 - L_{n})k_{nv}^{PY}, \quad \text{and}$$
$$k_{n}^{PB} = L_{n}k_{no}^{PB} + (1 - L_{n})k_{nv}^{PB}.$$

It is also assumed that only CheB-P can bind with the receptors, which leads to the equation relating different sub-species of CheB:

$$[B^{T}] = [B^{P}] + [B^{F}] - [B^{PF}]. \tag{20}$$

To describe the kinetics of the signal transduction pathway in full, we need to consider the interactions among the concentrations of all the 65 states for the four chemical species: 60 receptor states = two ligand binding states × five methylation states × three enzyme binding states × two phosphorylation states, one free CheR state, two free CheB states, and two CheY states. Using the fact that ligand-bind-

ing kinetics is fast and the enzymatic reactions are governed by Michaelis-Menten kinetics, the number of independent receptor concentrations is reduced from 60 to just 10, consisting of the five free methylation states and the five phosphorylation states. Now, the whole system is described by kinetic equations Eq. 10 and Eqs. 17–19, plus conservation equations given by Eqs. 7–9 and Eq. 20.

Concentration of the phosphorylated CheY ($[Y^{P}]$), which determines the tumbling frequency of bacteria, can be considered as the output of the whole chemotaxis signal transduction pathway. In the next section, we study how the steady state concentration of CheY-P depends on the external ligand concentration $[L]$; in particular, we derive a set of conditions for $[Y^{P}]$ to be independent of $[L]$, i.e., perfect adaptation.

## CONDITIONS FOR PERFECT ADAPTATION

All the concentrations in our model fall naturally into two categories: the local variables defined for one particular methylation level, such as $[T_{n}]$, which is the concentration of receptors with $n$-methyl groups, and the global variables, such as $[R^{F}]$, which is the concentration of the free CheR. The system adapts by adjusting the local variables with the ligand concentration, e.g., the steady-state values of $[T_{n}]$ varies with $[L]$. However, perfect adaptation is achieved when the equilibrium value of $[Y^{P}]$, a global variable, is independent of the ligand concentration (Othmer and Schaap, 1998). This is generally not possible because the global variables are coupled with the local ones. One goal of this article is to discover the conditions under which $[Y^{P}]$ becomes independent of $L$.

The strategy in obtaining the perfect adaptation conditions is to consider only global equations, such as the conservation equations of the chemical species (e.g., Eqs. 7, 8, and 20) and the steady-state equations of global variables (e.g., Eqs. 17 and 18), which do not depend on any one specific methylation level. In these global equations, there is no explicit dependence on ligand concentration, and composite variables, such as $\sum_{n=0}^{4}[T_{n}^{F}]/K_{n}^{R}$ in Eq. 7, enter as weighted sums of the methylation level specific receptor concentrations. Another kind of global equation can be constructed by summing steady-state equations at all methylation levels (e.g., Eqs. 9, 11, and 19). The price to pay for such global equations is the introduction of new composite variables. However, if the reaction rates involved in different reactions are related in certain ways, the same composite variables appear in different global equations so that there are enough global equations to determine all the independent global and composite variables. In other words, if certain conditions between reaction rates are satisfied, the steady-state concentrations of all the global and composite variables including $[Y^{P}]$ can be independent of the ligand concentration, i.e., perfect adaptation.

We leave the detailed derivation for the perfect adaptation conditions to the Appendix. In the following, we list these conditions, discuss their meaning and compare them with

those found in previous works (Barkai and Leibler, 1997; Yi et al., 2000). The perfect adaptation conditions can be grouped for each of the three pathway processes: condition 1 is for the ligand binding and unbinding, conditions 2–4 are required for the methylation process, and conditions 5–6 are related to the phosphorylation process:

1. The timescale for ligand binding is much shorter than the methylation and phosphorylation timescale. This condition allows us to neglect ligand-binding/unbinding kinetics.
2. The association rates between the receptor and the methylation/demethylation enzymes, CheR and CheB-P, are linearly related to the activity of the receptor and are zero for $n = 4$ and $n = 0$, respectively: $K_{n\lambda}^{R-1} \propto P_{4\lambda} - P_{n\lambda}$ and $K_{n\lambda}^{B-1} \propto P_{n\lambda} - P_{0\lambda}$. The dissociation rates of the enzyme receptor bound states are independent of $\lambda$.
3. The receptor activities of the nonmethylated and the maximally methylated receptors are independent of $\lambda$: $P_{0v} = P_{0o}$, $P_{4v} = P_{4o}$.
4. The ratios between the CheR catalytic rate $(k_n^R)$ and the CheB-P catalytic rate of the next methylation level $(k_{n+1}^B)$ are the same for all methylation states $n$: $k_{n+1}^B/k_n^R = $ const.
5. The phosphate transfer rates from CheA to CheB or CheY are proportional to CheA autophosphorylation rate: $k_{n\lambda}^{PB} \propto P_{n\lambda}$, $k_{n\lambda}^{PY} \propto P_{n\lambda}$.
6. The explicit dependence on $[T_n^F]$ distribution can be removed from the expression

$$\xi \equiv \left( -\frac{[R^F]}{K^R} + \frac{[B^{PF}]}{K^B} \right) \sum_{n=0}^{4} P_n^2 [T_n^F]. \qquad (21)$$

This condition can only be strictly satisfied when $[R^F]/(K^R) = [B^{PF}]/K^B$.

Condition 1 is necessary to decouple the ligand binding process from the rest of the reactions. This is verified experimentally and assumed in all the previous models (Barkai and Leibler, 1997; Morton-Firth and Bray, 1998; Spiro et al., 1997; Yi et al., 2000).

Condition 2 for the methylation process requires that the CheR and CheB methylation/demethylation rates depend linearly on the receptor's autophosphorylation rate (activity). This is a generalization of the key ingredient for perfect adaptation found in Barkai and Leibler's work (Barkai and Leibler, 1997). In the special case of $P_{4\lambda} = 1$ and $P_{0\lambda} = 0$, condition 2 means that CheB-P only binds to active receptors and CheR only binds to inactive receptors; the latter is missed in the original work of Barkai and Leibler, and was later found to be necessary for perfect adaptation in Morton-Firth et al. (1999), through a direct numerical simulation of the full system.

The requirement in condition 3 that $P_{0\lambda}$ and $P_{4\lambda}$ be independent of $\lambda$ is needed so that both the ligand-bound and vacant receptors have the same range of activity. This

requirement for perfect adaptation is necessary in case the extreme methylation states, $n = 0$ or $n = 4$, become populated with receptors.

Condition 4 was first pointed out in Yi et al. (2000). It is a more general form of the assumption that both $k_n^R$ and $k_n^B$ are independent of $n$ made in the original BL model. The justification of this condition may be related to a common evolutionary origin of CheR and CheB, resulting in a similar anchoring position to the receptor for CheR methylating site $n$ and CheB-P demethylating site $n + 1$ (Shapiro and Koshland, Jr., 1994; Shapiro et al., 1995; Djordjevic et al., 1998; Barnakov et al., 1999).

Condition 5 for the phosphorylation process is very similar to condition 2, in the sense that the phosphate transfer rates of the receptors have to be linearly related to their activity. This condition was not discovered before because the phosphorylation process was neglected in previous works (Barkai and Leibler, 1997; Yi et al., 2000).

Condition 6 can only be satisfied exactly when one tunes the parameters such that the prefactor in front of the sum in Eq. 21 is zero. This condition was overlooked by most of the previous studies because the activities of the CheR- or CheB-P-bound receptors were neglected. However, in equilibrium, the population of enzyme-bound receptors can be as high as 30% (Morton-Firth et al., 1999).

By imposing all the conditions above, the steady-state concentrations of the global variables will be independent of the ligand concentration, and are determined by 15 parameters: the four total concentrations of Tables 1 and 2, and the reaction rates of Table 3, including $P_4$ and $P_0$, but not the relative activity values for the rest of the methylation states. However, for real biological systems, these conditions for perfect adaptation may not be strictly satisfied. To understand bacteria's ability in adapting accurately under different internal and external conditions, i.e., robustness, we need to evaluate the effect of violating these perfect adaptation conditions.

## EFFECTS OF VIOLATING THE PERFECT ADAPTATION CONDITIONS

Since it is not feasible to explore the whole parameter space, we choose to mostly perturb around the parameter values that have been used in previous studies. To this end, we take most of our parameters from Morton-Firth et al. (1999), which are listed here in Tables 2 and 3. Hereafter we refer to this set of parameters as the reference parameters. Assuming ligand occupancy rate $L_n = L$ is independent of $n$, the steady-state receptor distributions in different methylation states for different ligand occupancy rates $L$ is shown in Fig. 2 A for the reference parameters. In Fig. 2 B, the population-weighted average receptor activities $P_n(L) = P_{no}L + P_{nv}(1 - L)$ for methylation level $n \in [0,4]$ is also shown. As is clear from Fig. 2, when ligand (attractant) occupancy rate increases, the average receptor activity $P_n(L)$ decreases for

**TABLE 3  System parameters and numerical values from Morton-Firth et al. (1999)**

| Symbol | Description | | 0 | 1 | 2 | 3 | 4 |
|--------|-------------|---|---|---|---|---|---|
| $P_{n\lambda}$ | Relative activity of $T_{n\lambda}$ | $v$ | 0 | 0.125 | 0.5 | 0.874 | 1 |
| | | $o$ | 0 | 0.017 | 0.125 | 0.5 | 1 |
| $K^R$ | CheR Michaelis constant | | | | | | 0.364 $\mu$M |
| $K^B$ | CheB Michaelis constant | | | | | | 1.405 $\mu$M |
| $k^R$ | CheR catalytic constant | | | | | | 0.819 s$^{-1}$ |
| $k^B$ | CheB catalytic constant | | | | | | 0.155 s$^{-1}$ |
| $k^P$ | CheA autophosphorylation rate | | | | | | 15.5 s$^{-1}$ |
| $k^{PY}$ | CheA $\rightarrow$ CheY phosphorus transfer rate | | | | | | 5 $\mu$M$^{-1}$ s$^{-1}$ |
| $k^{PB}$ | CheA $\rightarrow$ CheB phosphorus transfer rate | | | | | | 5 $\mu$M$^{-1}$ s$^{-1}$ |
| $k^{HY}$ | CheY dephosphorylation rate | | | | | | 14.15 s$^{-1}$ |
| $k^{HB}$ | CheB dephosphorylation rate | | | | | | 0.35 s$^{-1}$ |

each methylation level $n$, and the system adapts by shifting the receptor population toward higher methylation states in achieving constant total activity $[T^A] = \sum_{n=0}^{4} P_n(L)[T_n]$. The steady-state concentrations of all the other relevant concentrations at three different ligand occupancy fractions are given in Table 4 for the reference parameters. The small changes in $[Y^P]$ at different ligand concentrations are caused by violation of conditions 5 and 6 in the reference model used in Morton-Firth et al. (1999), as we explain later in the section Violating Condition 5.

We have also constructed another model by modifying some of the reference parameters so that all the perfect conditions are satisfied. The results of perturbing this new model are essentially the same as for the reference model, mainly because the adaptation error in the reference model is very small ($<1\%$). While this new model is mathematically more rigorous for isolating different error sources, the reference model has the advantage that it is motivated biologically (from experiments or common sense), and therefore serves as a better starting point in exploring the parameter regions that are more likely to be biologically relevant. To make sure violation of conditions 5 and 6 in the reference model does not contaminate the effect of other conditions too much, we have always checked the error with and without violating the condition in consideration, and made sure most

of the error does come from violating the perfect condition we study.

Since ligand binding is much faster than other relevant processes of the system, we do not consider the unrealistic situation of violating condition 1. In the following, we study the effects of breaking the other five perfect adaptation conditions. Our goal is to understand the general reason behind the robustness of the system with respect to breaking each perfect adaptation condition. Even though we primarily perturb the system around the reference parameters, we also explore other parameter regions, especially when the reference model becomes insensitive to violation of a given condition. This strategy allows us to gain the general understanding of where in the parameter space a given perfect adaptation condition becomes important and the reason behind it.

## Violation of condition 2

Condition 2 requires that the methylation/demethylation enzyme binding rates to a receptor depend linearly on the activity of the receptor. For the reference parameters, where $P_0 = 0$ and $P_4 = 1$, condition 2 simply means that CheR only binds to inactive receptors and CheB-P only binds to active receptors. The simplest way in violating condition 2 is to
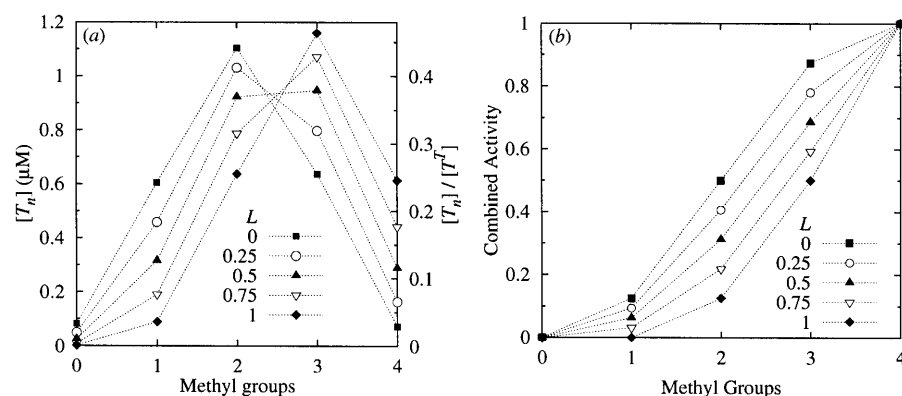


FIGURE 2 (a) Distribution of receptors in different methylation states at different ligand occupancy fractions $L$ for the reference parameters, with the total activity of the system being $[T^A] = 0.5[T^T]$. (b) The population-weighted average receptor activity $P_n(L)$ for different methylation levels $n \in [0,4]$ at different fractional ligand occupancy rates $L$.

**TABLE 4  Protein concentrations (in $\mu$M) at different ligand occupancy rates $L$ for the reference parameters**

| Species | $L = 0$ | $L = 0.5$ | $L = 1$ |
|---------|---------|-----------|---------|
| $[T_0]$ | 0.028 | 0.025 | 0.002 |
| $[T_1]$ | 0.605 | 0.316 | 0.089 |
| $[T_2]$ | 1.104 | 0.923 | 0.637 |
| $[T_3]$ | 0.637 | 0.947 | 1.159 |
| $[T_4]$ | 0.072 | 0.289 | 0.613 |
| $[T^A]$ | 1.257 | 1.250 | 1.274 |
| $[T^P]$ | 0.202 | 0.201 | 0.204 |
| $[R^F]$ | 0.050 | 0.050 | 0.050 |
| $[B^F]$ | 1.603 | 1.602 | 1.603 |
| $[B^{PT}]$ | 1.858 | 1.857 | 1.860 |
| $[B^{PF}]$ | 1.191 | 1.190 | 1.193 |
| $[Y^P]$ | 1.200 | 1.196 | 1.209 |

allow CheR to bind to active receptors or CheB-P to bind to inactive ones, which can be formally expressed as

$$K_{n\lambda}^{R-1} = K^{R-1} b_r (1 - P_{n\lambda} + a_r),$$
$$K_{n\lambda}^{B-1} = K^{B-1} b_b (P_{n\lambda} + a_b), \qquad (22)$$

where $a_r \geq 0$ and $a_b \geq 0$ are the measures of violating condition 2, and $b_r$ and $b_b$ are normalization factors tuned with respect to $a_r$ and $a_b$ to keep the total activity of the system constant at a given ligand occupancy rate ($L = 0.5$) for comparison purpose. Here, $a_r = 0$ and $a_b = 0$ correspond to condition 2 being satisfied; $a_r \to \infty$ (with $a_r b_r = const.$) or $a_b \to \infty$ (with $a_b b_b = const.$), respectively, corresponds to CheR or CheB-P binding to all receptors equally.

In Fig. 3, $A$ and $B$, we show the steady-state concentration of CheY-P versus the ligand occupancy rate $L$ for various values of $a_r$ and $a_b$ with the reference parameters. Even for the extreme cases of $a_r = \infty$ or $a_b = \infty$, respectively corresponding to CheR or CheB-P binding to both active and inactive receptors equally, the deviation from perfect adaptation is only $\sim 10-15\%$. Intuitively, the reason for the near-perfect adaptation is that the control of the system's total activity can be carried out by either the methylation (CheR) or demethylation (CheB-P) process, provided that at least one of the enzymes' binding rates is strongly correlated with the receptor activity. If the receptor binding rates of both enzymes become independent of the receptor's activity, i.e., both $a_r = \infty$ and $a_b = \infty$, the system is only controlled through the weak effect of CheB phosphorylation and does not adapt very well.

Specifically, condition 2 requires that CheR does not bind to the fully methylated receptors ($n = 4$), and CheB-P does not bind to the unmethylated receptors ($n = 0$). Therefore, the quantitative effects of breaking condition 2 (as in Eq. 22) depends on the receptor concentration at the fully methylated state $[T_4]$ or the unmethylated states $[T_0]$ (see Appendix for details). Both $[T_0]$ and $[T_4]$ are relatively small for the reference parameters with $[T_4] > [T_0]$ (see Fig. 2), which explains the qualitative features in Fig. 3, $A$ and $B$. The effect of $a_b \to \infty$ only becomes noticeable because $[T_0]$ is not too small for $a_b \to \infty$.

To test our prediction, we have studied our model with two new sets of parameters where $K^R$ and $K^B$ are changed
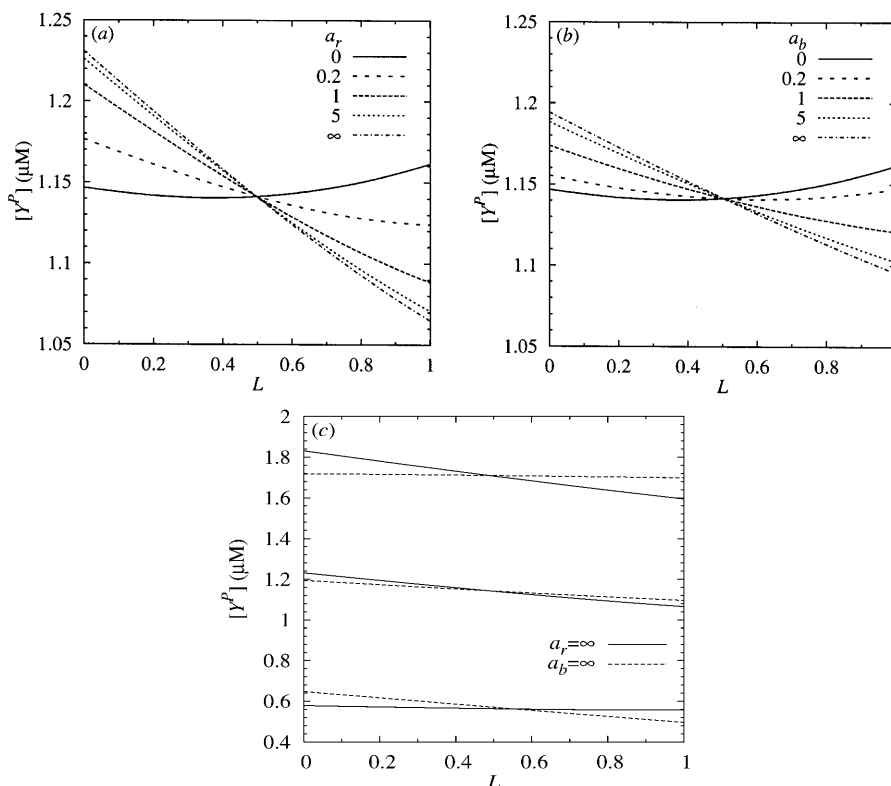


FIGURE 3  The steady-state $[Y^P]$ concentration versus ligand binding rate $L$ for different ways of breaking condition 2: ($a$) CheB-P binds with active receptors only ($a_b = 0$); CheR is allowed to bind with active receptor with varying strength $a_r = 0, 0.2, 1, 5$, and $\infty$, and where $a_r = \infty$ corresponds to CheR, binds to all receptor indiscriminately. ($b$) CheR binds with inactive receptors only ($a_r = 0$); CheB-P is allowed to bind with inactive receptor with varying strength $a_b = 0, 0.2, 1, 5$, and $\infty$, and where $a_b = \infty$ corresponds to CheB-P, binds to all receptor indiscriminately. ($c$) Two special cases of violating condition 2: $a_r = \infty$, $a_b = 0$ (*solid lines*), and $a_r = 0$, $a_b = \infty$ (*dotted lines*), are shown for two more sets of parameters in addition to the reference parameters. The parameters are chosen respectively to have the system's activities be higher (*upper curves*) or lower (*lower curves*) by 50% at $L = 1/2$ compared with that of the reference system (*middle curves*). For the system with lower activity, $[T_0]$ is larger; therefore, the effect of $a_b \to \infty$ is relatively bigger. For the system with higher activity, where $[T_4]$ is larger, the effect of $a_b \to \infty$ is relatively bigger.

away from their reference values, and tested the effect of violating condition 2 with these new parameters. The changes in $K^R$ and $K^B$ are chosen to make the new systems have higher (150%) and lower (50%) total activity, respectively, to compare with the reference system at a given receptor occupancy ($L = 1/2$) as shown in Fig. 3 C. For the system with lower activity, $[T_0]$ is larger; therefore the effect of $a_b \to \infty$ should be relatively bigger. For the system with higher activity where $[T_4]$ is larger, the effect of $a_r \to \infty$ should, therefore, be relatively bigger. These predictions are consistent with the numerical results shown in Fig. 3 C.

## Violation of condition 3

Since adaptation for bacterial chemotaxis relies on balancing the effect of ligand binding on the receptor's activity with that of the methylation of the receptor, a necessary condition for perfect adaptation is for both ligand-bound and vacant receptors to have the same range of activity, i.e., condition 3. For the reference parameters, condition 3 is obeyed by having: $P_{0v} = P_{0o} = 0$, and $P_{4v} = P_{4o} = 1$. Without changing the monotonic dependence of the receptor activity on their methylation level, we can break condition 3 at $n = 0$ by increasing $P_{0v}$ from 0 to 1/8; or at $n = 4$ by decreasing $P_{4o}$ from 1 to 7/8. The enzyme binding rates are adjusted accordingly in keeping condition 2 satisfied. The effects are shown in Fig. 4 A. The system is insensitive to the opening of the activity gap $\Delta P_0 \equiv P_{0v} - P_{0o}$ at $n = 0$, because the receptor population is small at $n = 0$ even at $L = 0$. For the same opening of activity gap $\Delta P_4 \equiv P_{4v} - P_{4o}$ at $n = 4$, the adaptation error is 6%. In particular, the system has a lower CheY-P concentration at the higher ligand occupancy rate $L$, because the receptor population shifts toward higher methylation levels at larger $L$, and the effect of methylation is not large enough to cancel the decrease of activity caused

by ligand binding. Quantitatively, the adaptation error increases with the activity gap; e.g., it reaches 25% when we lower $P_{4o}$ further to 0.5.

To verify the dependence of the effect of violating condition 3 on the receptor population, we have studied the behavior of our model with two new sets of parameters in addition to the reference parameters by increasing and decreasing the CheB Michaelis constant $K^B$ with respect to its reference value. For smaller $K^B (= 0.2K^B_{ref})$, the system has lower activity and $[T_0]$ is larger; therefore the effect of opening the receptor activity gap at $n = 0$ (i.e., $\Delta P_0$) should be larger. For larger $K^B (= 2K^B_{ref})$, the system has higher activity; $[T_4]$ is larger, therefore the effect of opening the receptor activity gap at $n = 4$ (i.e., $\Delta P_4$) should be larger. These predictions are again consistent with the results shown in Fig. 4 B.

## Violation of condition 4

The methylation and demethylation catalytic rates $k^R_n$ and $k^B_n$ can depend on methylation level $n$. From Eq. 11, the steady-state properties of the system only depend on the ratios: $r_n = k^B_n / k^R_{n-1}$ for $n = 1, 2, 3,$ and 4. Condition 4 for perfect adaptation requires that $r_n$ be a constant independent of $n$, a kind of detailed balance condition. Indeed, if we change $k^R_n$ and $k^B_n$ while keeping $r_n$ constant, the system adapts perfectly. However, when we make $r_n$ depend on $n$, perfect adaptation is lost. In Fig. 5, we show the effects of increasing one $r_n$ by a factor of 2 while keeping the other three $r_n$ constants unchanged at their reference value for $n = 1, 2, 3,$ and 4, respectively, for three sets of parameters. The quantitative deviation from perfect adaptation depends on $n$. As shown in Fig. 5, for the reference parameters (*middle curves*), the largest deviation of ~25% occurs at $n = 2$, possibly because the receptors are highly populated at $n = 2$ for the reference parameters.
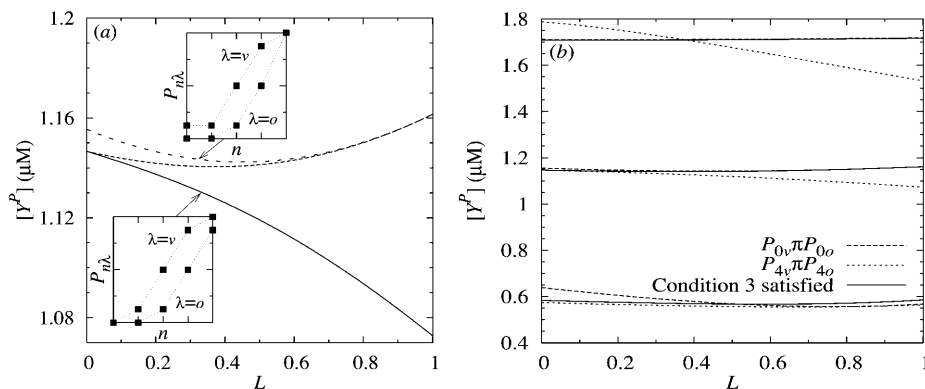


FIGURE 4 (*a*) The steady-state $[Y^P]$ concentration versus ligand occupancy fraction $L$ for different ways of breaking condition 3 by opening the activity gap at $n = 0$: $P_{ov} = P_{1v} = 1/8$ (*long dashed line*) or at $n = 4$: $P_{4o} = P_{3v} = 7/8$ (*short dashed line*), the solid line is for the reference parameters. The two inserts illustrate the opening of the activity gap at $n = 0$ and $n = 4$ respectively. (*b*) The effects of violating condition 3 in the same way as in left side of figure, with two more parameter sets: $K^B = 2K^B_{ref}$ (*upper curves*) and $K^B = 0.2K^B_{ref}$ (*upper curves*), in addition to the reference parameters (*middle curves*). For the new system with lower activity, where $[T_0]$ is larger, the effect of opening the activity gap at $n = 0$ is therefore larger. For the other new system with higher activity, where $[T_4]$ is larger, the effect of opening the activity gap at $n = 4$ is therefore larger.
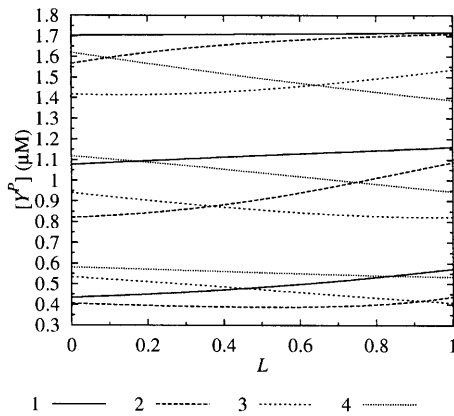
FIGURE 5 Steady-state CheY-P concentration $[Y^P]$ versus ligand occupancy rate $L$ for breaking condition 4 for three sets of parameters. The results are obtained by increasing one of the four ratios of catalytic rates (see text for definition) by a factor of 2: $r_n = 2r_{ref} = 0.38$, while keeping the other three ratios unchanged at the reference value of 0.19. The four different line types correspond to $n = 1, 2, 3$, and 4, respectively. In addition to the reference parameters (*middle curves*), two more sets of parameters are used, with $K^B = 2K_{ref}^B$ (*upper curves*) and $K^B = 0.2K_{ref}^B$ (*lower curves*). For the reference parameters, violation of condition 4 with $n = 2$ has the largest effect. For the new systems with higher $K^B = 2K_{ref}^B$ and lower $K^B = 0.2K_{ref}^B$ activities, the effect of violating condition 4 is more severe at a larger ($n = 4$) and a smaller ($n = 1$) methylation level, respectively, because of the changes in the receptor population distribution.

To demonstrate the dependence of the effects of violating condition 4 on the receptor population distribution, we have studied two other set of parameters with $K^B = 2K_{ref}^B$ and $K^B = 0.2K_{ref}^B$ (the same as used in Fig. 4 *B*) in addition to the reference parameters. As shown in Fig. 5, for the new systems with higher ($K^B = 2K_{ref}^B$, *upper curves*) and lower ($K^B = 0.2K_{ref}^B$, *lower curves*) activities, the effect of violating condition 4 is most severe at a larger ($n = 4$) and a smaller ($n = 1$) methylation level, respectively, because of the changes in the receptor population distribution, among different methylation levels, caused by the different values of $K^B$.

## Violation of condition 5

Condition 5 requires that the phosphate transfer rates of a receptor be proportional to its autophosphorylation rate, a kind of compatibility condition. The simplest way to break condition 5 is to set the phosphate transfer rates to be a constant independent of both the ligand binding and the methylation level of the receptor. This assumption is also made in Morton-Firth and Bray (1998), and Morton-Firth et al. (1999).

For the reference parameters, the steady-state $[Y^P]$ change by less than 1% over the whole range of ligand occupancy as shown in Fig. 6 (*curve a*), indicating the insensitivity of the system's perfect adaptation with respect to this particular choice of breaking condition 5. In the following, we explain the system's near-perfect adaptation by the existence of approximate global equations.
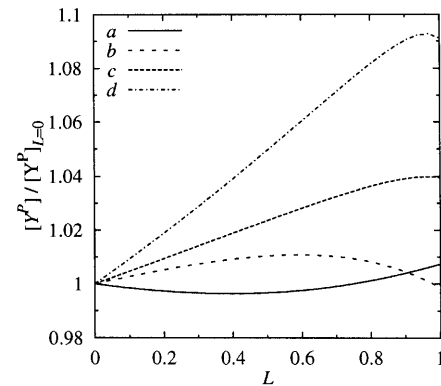


FIGURE 6 Relative steady-state CheY-P concentrations $[Y^P]/[Y^P]_{L=0}$ versus ligand occupancy rate $L$ when condition 5 is violated; the adaptation error depends on the parameters of the system, four cases are studied here using parameters with increasing degrees of deviation from their reference values (see text for detail). The parameters used are: for curve $a$, reference parameter values; for curve $b$, same as for curve $a$, except $[Y^T] = [Y^T]Ref/20$; for curve $c$, same as for curve $b$, except $k^R = k^R Ref/50$; and for curve $d$, same as for curve $c$, except $P_{v1} = 0.25$ and $P_{v2} = 0.6$.

In deriving condition 5, a global equation is formed by summing Eq. 19 over all methylation levels and replacing $[T_n^U]$ by $[T_n] - [T_n^P]$, which leads to the formation of four composite variables: $G_0 = \sum_{n=0}^{4} k_n^P[T_n]$, $G_1 = \sum_{n=0}^{4} k_n^P[T_n^P]$, $G_2 = \sum_{n=0}^{4} k_n^{PY}[T_n^P]$, and $G_3 = \sum_{n=0}^{4} k_n^{PB}[T_n^P]$. Condition 5 is needed to make $G_1$, $G_2$, and $G_3$ proportional to each other, so that the total number of global equations is enough to solve for all the independent global and composite variables (see section Conditions for Perfect Adaptations, and Appendix, for details). When condition 5 is broken by setting $k_n^{PB}$ and $k_n^{PY}$ to be constant, $G_2$ and $G_3$ are still proportional to each other; but as they are now different from $G_1$, the total number of global equations are now not enough in solving for all the global variables, and local equations have to be used. This leads to all the global variables dependent upon ligand concentration; i.e., nonperfect adaptation. However, because the concentration of (unphosphorylated) CheY is much larger than the receptor concentrations, the phosphorylated receptor concentration $[T_n^P]$ is small compared with the total receptor concentration $[T_n]$, due to efficient phosphate transfer from CheA to CheY and the subsequent high CheY-P dephosphorylation rate. As a result, $G_1$ is negligible relative to $G_0$, leading to an approximate global equation with the same degree of reduction in independent composite variables and eventually the near-perfect adaptation observed in Fig. 6 (*curve a*).

However, reducing CheY concentration alone does not change too much the system's ability in perfect adaptation, as shown in Fig. 6 (*curve b*). At low CheY concentration, the phosphate group of CheA-P goes to CheB. Because of the slow dephosphorylation rate of CheB-P, most of the CheB become phosphorylated in steady state, essentially decoupling the phosphorylation process from the adaptation process. The adaptation of the system therefore becomes insensitive to the phosphorylation-related condition 5.

To amplify the effect of violating condition 5, we reduce the overall activity to $[T^A] = 0.014[T^T]$ at $L = 0$ by making $k^R = 0.02k_{Ref}^R$. The result is shown in Fig. 6 (*curve c*). The adaptation accuracy can also depend on other parameters, such as the receptor activity $P_{n\lambda}$. In Fig. 6 (*curve d*), we show that a slight change in receptor activity leads to higher deviation from perfect adaptation.

## Violating condition 6

The total receptor activity $[T^A](\equiv \sum_{n=0}^{4} P_n[T_n])$ is directly related to the final production of CheY-P. However, only part of $[T^A]$ can be expressed in terms of other composite variables related to receptor population, i.e., the total free receptor concentration $[T^F] \equiv \sum_{n=0}^{4}[T_n^F]$ and the total activity due to free receptors $[T^{AF}] \equiv \sum_{n=0}^{4} P_n[T_n^F]$. It has an extra term $\xi$ coming from the activity of the enzyme (CheR or CheB-P)-bound receptors (see Appendix for details), which is proportional to $\xi' = \sum_{n=0}^{4} P_n^2[T_n^F]$ with a prefactor $(-[R^F]/K^R) + ([B^{PF}]/K^B)$ (see Eq. 21). Condition 6 is required to eliminate this extra global variable $\xi'$ by setting the prefactor to zero.

The effect of breaking condition 6 can be small, because as $[R^F]$ deviates from its perfect adaptation value $[R^F]_{Adap}$, so does $[B^{PF}]$ with the same trend, leading to small changes of the prefactor in $\xi$. Also, part of $\xi'$ can be approximated by a linear combination of $[T^F]$ and $[T^{AF}]$, depending on the activity levels of different receptors $P_{n\lambda}$. Finally, for higher total activity, the relative effect of $\xi$ will be small. For the reference parameters, the accuracy of adaptation is better than 98% for fourfold change of CheR concentration from its perfect adaptation value, as shown in Fig. 7 *A*. The adaptation accuracy decreases as we lower the total activity by decreasing methylation rate $k^R$, as shown in Fig. 7 *B*. Finally, when we increase the activity differences between the ligand-bound and the vacant receptors by setting: $P_{no} = 0$ ($n = 0, 1, 2,$ and 3), $P_{4o} = 1$; and $P_{nv} = 1$ ($n = 1, 2, 3,$ and 4), $P_{0v} = 0$, the same change in $[R^T]$ can cause more than a 50% error in adaptation, as shown in Fig. 7 *C*.

## COMPARISON TO STOCHASTIC SIMULATION AND EXPERIMENTS

The results from the previous sections can be compared with both the discrete stochastic numerical simulation and real experiments. We use the reference parameters for all the comparison studies.

## Comparison to stochastic simulation

Stochsim (Morton-Firth and Bray, 1998) is a general purpose stochastic simulator for chemical reactions. For our study, the volume of Stochsim simulation is set to be $1.4 \times 10^{-15} L$, and the number of molecules is therefore $843 \times$ concentration (in $\mu M$).

In Fig. 8 *A*, we show the Stochsim simulation result for the reference parameters, which agrees well with the results from
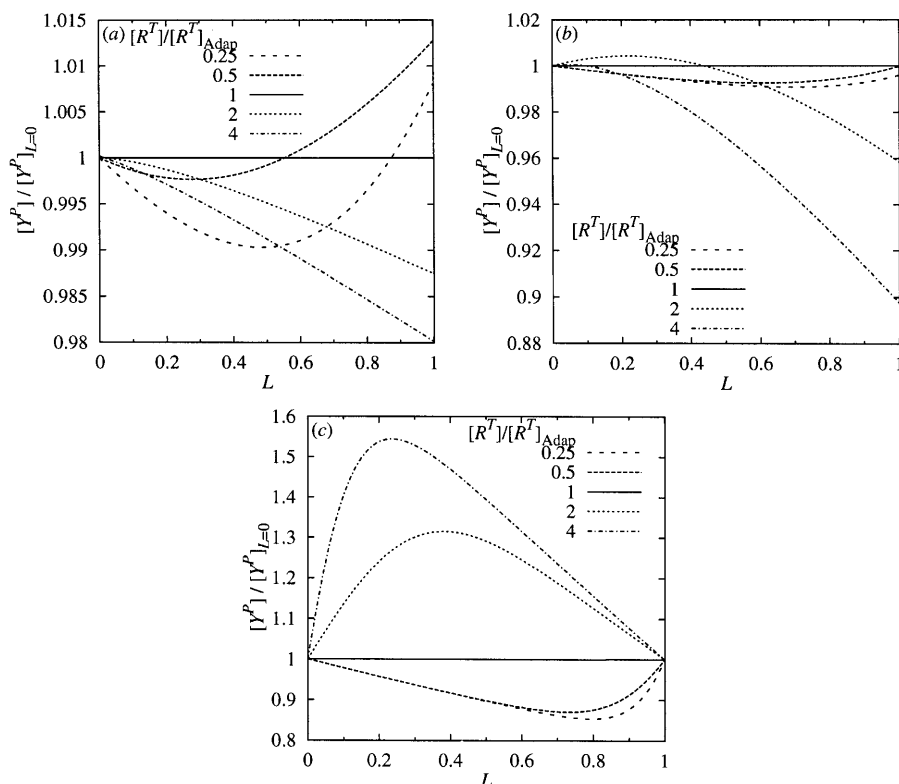


FIGURE 7 Relative steady-state CheY-P concentrations $[Y^P]/[Y^P]_{L=0}$ versus ligand occupancy rate for different CheR concentrations (with condition 5 satisfied), which are varied with respect to the perfect adaptation value $[R^T]_{Adap}$: (*a*) Reference parameters are used except the different values of $[R^T]$ listed in the figure, and $[R^T]_{Adap} = 2.63[R^T]_{ref}$; (*b*) $K^R = 0.1K_{ref}^R$ is chosen in reducing the total activity, where adaptation is less accurate, and $[R^T]_{Adap} = 5.26[R^T]_{ref}$; and (*c*) Same parameters as in *B*, except that the activity difference between ligand-bound and vacant receptors are set to be maximum (see text), and $[R^T]_{Adap} = 5.35[R^T]_{ref}$.
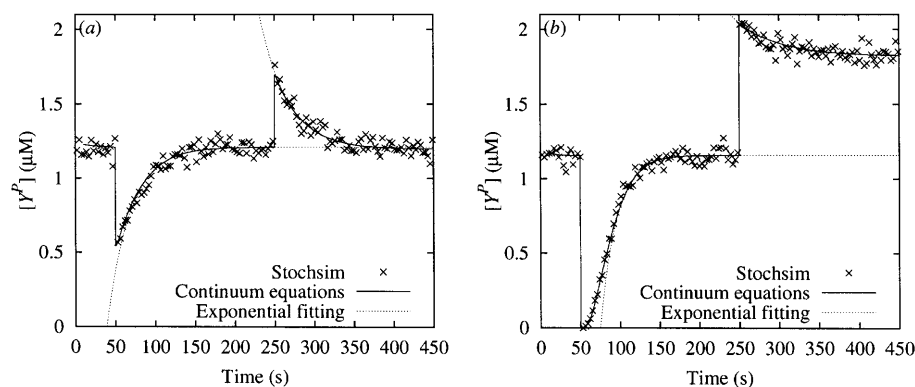
FIGURE 8 Dynamics of $[Y^P]$ from Stochsim simulation with ligand occupancy rates $L$ changing from $0 \rightarrow 1 \rightarrow 0.2$ at 50 and 250 s when the parameters are set to: (a) the reference values, and (b) same as in Fig. 7 C with $[R^T] = 4[R^T]_{Adap}$. The solid lines are results from simulations of our deterministic equations; the dotted lines are fits to the Stochsim data with an exponential decaying function to obtain the relaxation time.

simulating our continuum equations with the same parameters. In Fig. 8 B, we show the Stochsim simulation result for the parameters used in Fig. 7 C with $[R^T] = 4[R^T]_{Adap}$, where perfect adaptation is lost because of violation of condition 6. As predicted from our deterministic model, after sudden changes of ligand occupancy rate $L$, $[Y^P]$ does not always return to its prestimulus level; in fact, the maximum error ($\sim 50\%$) is observed when $L = 0.2$, consistent with Fig. 7 C.

For most of the results shown in this article, we have compared with the results from stochastic simulation using Stochsim (data not shown). Overall, the averaged behaviors of Stochsim simulations are consistent with our continuum model, which is interesting given the nonlinear nature of the chemical kinetics. Further work is needed in characterizing the fluctuation of the individual Stochsim simulations, and in comparing them with the fluctuations in behavior among different individual bacteria (Morton-Firth and Bray, 1998).

## Comparison with experiment

In a recent experimental study by Alon and co-workers (Alon et al., 1999), mutant bacteria lacking a certain chemotaxis protein, such as CheR, CheB, CheY, or CheZ, are used, and the missing protein is reintroduced in a controlled fashion through a plasmid inserted into the mutant bacteria cells. This technique allowed these authors to study the effect of various enzyme concentration changes

on the chemotaxis behavior of the bacteria. Specifically, the tumbling frequency of the bacteria is measured through a sudden increase of ligand concentration, which effectively corresponds to a sudden change of ligand occupancy rate from $L = 0$ to $L = 1$.

In Fig. 9 A, we show the adaptation precision as the ratio between phosphorylated CheY level before and after the stimulus for various CheR and CheB concentrations. For CheR concentration change of up to 50-fold with respect to the reference value, the adaptation error is $<3\%$, somewhat smaller than the experimentally measured adaptation error cited in Alon et al. (1999). If $[B^T]$ instead of $[R^T]$ is changed, the adaptation error would be much bigger, as shown in Fig. 9 A. This is the case because for large values of $[B^T]$, the low activity and the large values of $[B^{PF}]$ make the violation of condition 5 and 6 more significant. This could explain the larger (1.09) adaptation precision reported in Alon et al. (1999) when $[B^T]$ expression is 12 times that of the wild-type values. Since we define adaptation accuracy based on CheY-P concentration, the quantitative difference between the adaptation error observed in Alon et al. (1999) and those of our model could be explained by the signal amplification at the motor level (Cluzel et al., 2000).

The relaxation time of the system after a sudden change in ligand concentration can be determined by direct simulation of the full kinetic equation or by linearizing the methylation/demethylation kinetic equations around the steady state. The
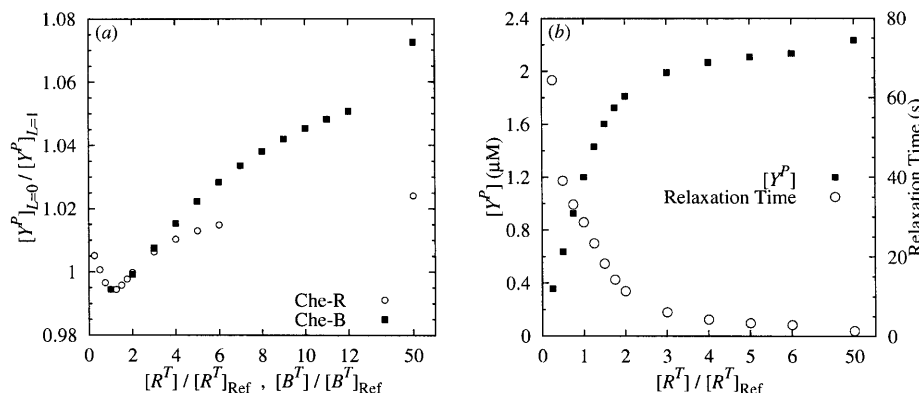


FIGURE 9 The response to a sudden increase of ligand concentration determined from the continuum model. (a) The steady-state CheY-P concentration ratios before and after the stimulus, $[Y^P]_{L=0}/[Y^P]_{L=1}$, for different fold changes of CheR or CheB concentrations; and (b) steady-state CheY-P concentration and the linear relaxation time upon sudden change of ligand occupancy rate (from 0 to 1) versus different CheR concentrations.

dependence of both the steady-state tumbling frequency and the linear relaxation time on CheR concentration $[R^T]$ is shown in Fig. 9 *B*. They agree qualitatively with the steady-state tumbling frequency and the relaxation time measured in Alon et al. (1999), as depicted in Fig. 2 *B* of their article, although direct quantitative comparison is not possible due to different definitions of relaxation time and lack of detailed understanding on how CheY-P regulates the motor.

## DISCUSSIONS AND CONCLUSIONS

In this article, we have studied a theoretical model describing the full chemotaxis signal transduction pathway. Through systematic analysis of the steady-state properties of the model, we derive a complete set of conditions for the system to adapt exactly. Some of the conditions are generalizations of the ones discovered before, but others—in particular, the conditions related to the phosphorylation part of the pathway—are discovered for the first time here. It is quite remarkable that perfect adaptation can be achieved for arbitrary ligand concentration with a small set of conditions, far less than the number of variables and the number of reaction rate constants in the problem.

The (intrinsic) state of a receptor can be described by its ligand-binding status ($\lambda$) and methylation level (*n*). The (external) properties of the receptor complex include its abilities to interact with the methylation/demethylation enzymes, to undergo autophosphorylation, and to transfer its own phosphate group to CheY or CheB, all of which depends on the (internal) state of the receptor characterized by *n* and $\lambda$. Perfect adaptation requires these three properties of the receptor complex to be correlated with each other in a linear fashion for any given receptor state $\{n\lambda\}$ (conditions 2 and 5). Available experimental data that addresses the validity of such connections has been discussed extensively in Yi et al. (2000). Even though the evidence for such connections is not well established and the correlation may not be linear, it is conceivable that a high degree of correlation exists among these three properties of the receptor, because they are determined by the same conformational change of the receptor protein complex for a given receptor state $\{n\lambda\}$.

Since most of the perfect adaptation conditions are relations between different reaction rates, the system's ability to adapt accurately can be considered robust in the sense that the perfect adaptation is independent of concentrations of any specific chemotaxis protein, which can fluctuate between different individual cells and at different stages of the cell development. Only one of the perfect adaptation conditions requires the fine-tuning of the methylation enzyme concentrations (condition 6). Because of this condition, in the strict mathematical sense, the perfect adaptation of the system can only be achieved via fine tuning of a parameter, and therefore cannot be considered robust. However, as we have shown in this article, the effect of violating this condition can be rather small, especially at the reference parameters.

The discovery of the perfect adaptation conditions provides an invaluable starting point in exploring the parameter space. We evaluate the sensitivity of the system's perfect adaptation ability by perturbing the perfect adaptation conditions. We find that the system can adapt near perfectly even in the absence of some of the perfect adaptation conditions. In finding the perfect adaptation conditions, we focus on studying equations which do not depend on any individual methylation levels; these global equations are obtained by either conservation laws or summing steady-state equations over different methylation levels. The same approach is also useful in understanding the near-perfect adaptation when the perfect adaptation conditions are violated. Technically, we can explain the near-perfect adaptation by the existence of approximate global equations replacing those lost due to the violation of perfect adaptation conditions. Biologically, these approximate global equations are caused by various intrinsic properties of the system, such as separation of scales in protein concentrations and reaction rates, or specific properties of the receptor distribution in different methylation states. Since real biological systems are not likely to satisfy all the perfect adaptation conditions exactly, the abundance of such near-perfect adaptation regions in the parameter space strongly limits the range of activity variation and is probably responsible for the robustness of the system's ability to adapt almost perfectly.

Through systematic study of the system's behavior when different perfect adaptation conditions are violated, we have also identified parameter regions where significant deviation from perfect adaptation occurs. This may provide possible explanations to bacterial chemotaxis responses that does not adapt accurately, such as the serine response as reported in Berg and Brown (1972), and constitute concrete predictions that can be experimentally verified.

Aside from perfect adaptation, another challenge for modeling bacterial chemotaxis is to understand the large signal amplification from ligand concentration change to the change in bacterium flagella rotation bias. To directly compare between experiments and simulation, detailed information between CheY-P concentration and the motor rotation bias is needed. Recently, the connection between CheY-P level and the motor activity was investigated in Scharf et al. (1998), Alon et al. (1998), and Cluzel et al. (2000). In the Cluzel study (Cluzel et al., 2000), where rotation bias of single bacterium was measured for different $[Y^P]$ concentrations, it was shown that the motor bias for individual bacterium should be fitted by a Hill function with a large Hill coefficient ($\sim$10). This highly nonlinear function may explain the advantage of perfect adaptation in amplifying the gain, and also the nonlinear dependence of BCCW, the CCW rotation bias, on changes in ligand occupancy as found in Jasuja et al. (1999). However, quantitatively, from Cluzel et al. (2000), the maximum signal amplification from change in $[Y^P]$ to the tumbling frequency is measured to be: $dB_{ccw}/d \ln[Y^P] \approx 2.2$. With the reference parameters in our model, this leads to a total signal amplification of $dB_{CCW}/d \ln[Y^P] \times d \ln[Y^P]/$

$dL \approx 2.2 \times 0.65 \approx 1.43$, which is still much too small as compared with the total signal amplification measured in experiments, e.g., $\sim 30$ as reported in Jasuja et al. (1999).

The gain of the system could come from receptor clustering as suggested in Bray et al. (1998). However, to reconcile the existence of high gain and the wide dynamic range of response, it is highly desirable to have high gain for the signal transduction pathway itself. One of the interesting findings of our study is that if the system satisfies all the perfect adaptation conditions, the steady-state activity of the system is independent of the exact values of the receptor activity $P_{n\lambda}$ for $n \in [1,3]$. On the other hand, the response of the system, defined here as the difference of CheY-P concentrations between its extreme value after the stimulus and its original value before the stimulus, directly depends on the difference of receptor activity between ligand-bound and ligand free receptors: $\Delta P_n \equiv P_{nv} - P_{no}$. The higher these differences are, the higher the response will be. To have high response, it is favorable to increase $\Delta P_n$ and to have lower total activity. Indeed, if we simply increase the activity difference between the ligand-bound and vacant receptor, such as those used in Fig. 7 $C$, the total amplification can be increased to: $2.2 \times 1.7 = 3.74$. Other changes, such as reducing the system's total activity, can enhance the gain much more, as noted also in Barkai et al. (2001). (A detailed study of the response of the system is outside the scope of this article, and will be reported in another communication.)

Overall, the current model is capable of explaining the qualitative behaviors of the chemotaxis pathway related to adaptation; in particular, the robustness of the system's ability to adapt nearly perfectly. Much work is still needed to modify and enrich the model to understand the high sensitivity and wide dynamic range of the system (Sourjik and Berg, 2002). However, because adaptation and response occur with very different timescale and via largely different molecular processes, modification of the model in explaining the high response gain should not change the perfect adaptation conditions significantly. Indeed, it is not hard to show that even with receptor coupling added to the current model, the conditions we identified in this article are still needed for the system to achieve perfect adaptation; the only change is that activity of each receptor now depends also on its neighbors' activities (B. Mello and Y. Tu, unpublished results). We believe that, as long as the basic structure of the protein interaction network stays intact, the perfect adaptation conditions identified here will be mostly valid. These conditions not only offer explanation for adaptation accuracy and its robustness. They also serve as constraints for constructing quantitative models in understanding other aspects of the bacterial chemotaxis.

## APPENDIX

In this section, we describe the detailed derivation of the perfect adaptation conditions listed in the section Conditions for Perfect Adaptation. As described there, the approach is to construct global equations using global and composite variables that do not depend on the receptor population in any one individual methylation state.

First, we concentrate on the methylation-related equations. Eqs. 7–8 and summation of Eq. 9 over $n \in [0,4]$ gives three global equations. For the steady state, the methylation flux between different methylation states should be zero:

$$J_n = k_n^R \frac{[R^F][T_n^F]}{K_n^R} - k_{n+1}^B \frac{[B^{PF}][T_{n+1}^F]}{K_{n+1}^B} = 0, \quad (0 \le n \le 3).$$ (23)

Condition 4 can be used in factoring out the common $n$-dependent factor from $K_{n+1}^R$ and $K_n^B$ in $J_n$, after which Eq. 23 is summed over $n \in [0,3]$ to obtain a global equation.

Using condition 2, the Michaelis constants can be expressed as $K_{n\lambda}^R = K^R/(P_{4\lambda} - P_{n\lambda})$ and $K_{n\lambda}^B = K^B/(P_{n\lambda} - P_{0\lambda})$, where $K^R$ and $K^B$ are constants. If we further enforce condition 3, i.e., $P_{4o} = P_{4v} \equiv P_4$ and $P_{0o} = P_{0v} \equiv P_0$, we can convert all the weighted sums of the individual receptor concentrations into two composite receptor concentrations $[T^F]$ and $[T^{AF}]$. $[T^F] \equiv \sum_{n=0}^{4}[T_n^F]$ is the total concentration of the free receptor, and $[T^{AF}] \equiv \sum_{n=0}^{4} P_n[T_n^F]$ is the total concentration of the active free receptors, where $P_n \equiv (1 - L_n)P_{nv} + L_nP_{no}$ is the population-weighted average activity for a receptor with $n$-methyl groups. Therefore, after applying conditions 2, 3 and 4, the four methylation-related global equations can be written as:

$$[R^T] = [R^F]\left(1 + P_4\frac{[T^F]}{K^R} - \frac{[T^{AF}]}{K^R}\right),$$ (24)

$$[B^P] = [B^{PF}]\left(1 - P_0\frac{[T^F]}{K^B} + \frac{[T^{AF}]}{K^B}\right),$$ (25)

$$[T^T] = \left(1 + P_4\frac{[R^F]}{K^R} - P_0\frac{[B^{PF}]}{K^B}\right)[T^F]$$
$$+ \left(-\frac{[R^F]}{K^R} + \frac{[B^{PF}]}{K^B}\right)[T^{AF}],$$ (26)

$$k^R[R^F]\frac{(P_4[T^F] - [T^{AF}])}{K^R} - k^B[B^{PF}]\frac{(-P_0[T^F] + [T^{AF}])}{K^B} = 0.$$ (27)

If $K_{n\lambda}^B$ is a constant (i.e., CheB-P binds equally to all receptors), condition 2 is violated. However, it is not hard to see that if the receptor population in the $n = 0$ methylation state, $[T_0]$, is small, we can still sum up the methylation balance equations to form a global equation. The same is true if $K_{n\lambda}^R$ is a constant and $[T_4] \approx 0$.

Next, we focus on the phosphorylation-related equations. Besides its importance in producing the final output of the signal transduction pathway CheY-P, the phosphorylation is also coupled back to the methylation process through concentration $[B^{PF}]$. By writing $k_{n\lambda}^P \equiv k^P P_{n\lambda}$ and using condition 5: $k_{n\lambda}^{PY} \equiv k^{PY} P_{n\lambda}$ and $k_{n\lambda}^{PB} \equiv k^{PB} P_{n\lambda}$, the phosphorylation-related global equations can be written as:

$$[Y^P] = \frac{k^{PY}[T^{PA}]}{k^{HY} + k^{PY}[T^{PA}]}[Y^T],$$ (28)

$$[B^{PF}] = \frac{k^{PB}[T^{PA}]}{k^{HB} + k^{PB}[T^{PA}]}[B^F],$$ (29)

$$[T^{PA}] = \frac{[T^A]}{1 + \frac{k^{PY}}{k^P}([Y^T] - [Y^P]) + \frac{k^{PB}}{k^P}([B^F] - [B^{PF}])}.$$ (30)

Eq. 30 is obtained by summing Eq. 19 over $n \in [0,4]$. There are two composite variables, $[T^{PA}]$ and $[T^A]$ in the above equations. $[T^A] \equiv \sum_{n=0}^{4} P_n[T_n]$ is the total concentration of active receptors; $[T^{PA}] \equiv \sum_{\lambda=v,o}^{n=0,4} P_{n\lambda}[T_{n\lambda}^P]$ is phosphorylated active receptor concentrations.

If the CheA phosphate transfer rates are independent of its ligand/methylation status, i.e., $k_{n\lambda}^{PY} \equiv k^{PY}$ and $k_{n\lambda}^{PB} \equiv k^{PB}$, condition 5 is broken. A new composite variable $[T^P] \equiv \sum_{n=0}^{4}[T_n^P]$ appears in the above equations, replacing $[T^{PA}]$ in Eqs. 28–29 and part of Eq. 30. However, if $[T^{PA}] \ll [T^A]$, e.g., due to efficient phosphate transfer from CheA to CheY, $[T^{PA}]$ can be neglected, and again, there will be only two composite variables in the phosphorylation-related global equations, and therefore the system may still adapt near-perfectly in absence of condition 5, as discussed in the section Violating Condition 5. The methylation and the phosphorylation global equations communicate through various CheB concentrations. An extra equation is necessary to connect the concentrations of these different forms of the same proteins:

$$[B^T] = [B^P] + [B^F] - [B^{PF}]. \tag{31}$$

Finally, by using Eq. 9, we can write down the expression for the total receptor activity of the system $[T^A]$ that appears in Eq. 30:

$$[T^A] = \sum_{n=0}^{4} P_n[T_n] = \left(1 + P_4 \frac{[R^F]}{K^R} - P_0 \frac{[B^{PF}]}{K^B}\right)[T^{AF}]$$
$$+ \left(-\frac{[R^F]}{K^R} + \frac{[B^{PF}]}{K^B}\right) \sum_{n=0}^{4} P_n^2[T_n^F]. \tag{32}$$

The above equation contains a new composite variable $\xi' = \sum_{n=0}^{4} P_n^2[T_n^F]$. Condition 6 is thus required to eliminate this extra term. Part of $\xi'$ can be expressed in terms of the other composite variables, such as $[T^F]$ and $[T^{AF}]$. Therefore, the effect of violating condition 6 cannot be simply measured by the value of $\xi'$, as we discussed in the section Violating Condition 6.

If all the conditions listed in Conditions for perfect adaptation are satisfied, we have nine global equations, Eqs. 24–32; these nine global equations contain five global variables: $[R^F]$, $[B^P]$, $[B^{PF}]$, $[B^F]$, and $[Y^P]$, and four composite variables: $[T^F]$, $[T^{AF}]$, $[T^A]$, and $[T^{PA}]$. Therefore, the steady-state values of all the nine global or composite variables, including $[Y^P]$, will be independent of the ligand concentration and the system can achieve perfect adaptation.

## REFERENCES

Alon, U., L. Camarena, M. G. Surette, B. Aguera y Arcas, Y. Liu, S. Leibler, and J. B. Stock.1998. Response regulator output in bacterial chemotaxis. *EMBO J.* 17:4238–4248.

Alon, U., M. G. Surette, N. Barkai, and S. Leibler. 1999. Robustness in bacterial chemotaxis. *Nature.* 397:168–171.

Asakura, S., and H. Honda. 1984. Two-state model for bacterial chemoreceptor proteins. The role of multiple methylation. *J. Mol. Biol.* 176: 349–367.

Barkai, N., and S. Leibler. 1997. Robustness in simple biochemical networks. *Nature.* 387:913–917.

Barkai, N., U. Alon, and S. Leibler. 2001. Robust amplification in adaptive signal transduction networks. *C. R. Acad. Sci. Paris.* 2:1–7.

Barnakov, A. N., L. A. Barnakova, and G. L. Hazelbauer. 1999. Efficient adaptational demethylation of chemoreceptors requires the same enzyme-docking site as efficient methylation. *Proc. Natl. Acad. Sci. USA.* 96:10667–10672.

Berg, H. C., and D. A. Brown. 1972. Chemotaxis in *Escherichia coli* analysed by three-dimensional tracking. *Nature.* 239:500–504.

Borkovich, K. A., L. A. Alex, and M. I. Simon. 1992. Attenuation of sensory receptor signaling by covalent modification. *Proc. Natl. Acad. Sci. USA.* 89:6756–6760.

Bornhorst, J. A., and J. J. Falke. 2001. Evidence that both ligand binding and covalent adaptation drive a two-state equilibrium in the aspartate receptor signaling complex. *J. Gen. Physiol.* 118:693–710.

Bourret, R. B., and A. M. Stock. 2002. Molecular information processing: lessons from bacterial chemotaxis. *J. Biol. Chem.* 277:9625–9628.

Bray, D., R. B. Bourret, and M. I. Simon. 1993. Computer simulation of the phosphorylation cascade controlling bacterial chemotaxis. *Mol. Biol. Cell.* 4:469–482.

Bray, D., M. D. Levin, and C. J. Morton-Firth. 1998. Receptor clustering as a cellular mechanism to control sensitivity. *Nature.* 393:85–88.

Bren, A., and M. Eisenbach. 2000. How signals are heard during bacterial chemotaxis: protein-protein interactions in sensory signal propagation. *J. Bacteriol.* 182:6865–6873.

Cluzel, P., M. Suette, and S. Leibler. 2000. An ultrasensitive bacterial motor revealed by monitoring signaling proteins in single cells. *Science.* 287:1652–1655.

Djordjevic, S., P. N. Goudreau, Q. Xu, A. M. Stock, and A. H. West. 1998. Structural basis for methylesterase CheB regulation by a phosphorylation-activated domain. *Proc. Natl. Acad. Sci. USA.* 95:1381–1386.

Dunten, P., and D. E. Koshland, Jr. 1991. Tuning the responsiveness of a sensory receptor via covalent modification. *J. Biol. Chem.* 266:1491–1496.

Falke, J. J., R. B. Bass, S. L. Butler, S. A. Chervitz, and N. A. Danielson. 1997. The two-component signaling pathway of bacterial chemotaxis. *Annu. Rev. Cell Dev. Biol.* 13:457–512.

Hauri, D. C., and J. Ross. 1995. A model of excitation and adaptation in bacterial chemotaxis. *Biophys. J.* 68:708–722.

Jasuja, R., Y. Lin, D. R. Trentham, and S. Khan. 1999. Response tuning in bacterial chemotaxis. *Proc. Natl. Acad. Sci. USA.* 96:11346–11351.

Liu, Y., M. Levit, R. Lurz, M. G. Surette, and J. B. Stock. 1997. Receptor-mediated protein kinase activation and the mechanism of transmembrane signaling in bacterial chemotaxis. *EMBO J.* 16:7231–7240.

Lukat, G. S., B. H. Lee, J. M. Mottonen, A. M. Stock, and J. B. Stock. 1991. Roles of the high conserved aspartate and lysine residues in the response regulator of bacterial chemotaxis. *J. Biol. Chem.* 266:8348–8354.

Morton-Firth, C. J., and D. Bray. 1998. Predicting temporal fluctuations in an intracellular signalling pathway. *J. Theor. Biol.* 192:117–128.

Morton-Firth, C. J., T. S. Shimizu, and D. Bray. 1999. A free-energy-based stochastic simulation of the tar receptor complex. *J. Mol. Biol.* 286:1059–1074.

Othmer, H. G., and P. Schaap. 1998. Oscillatory cAMP signaling in the development of *Dictyostelium discoideum. Comm. Theoret. Biol.* 5:175–282.

Scharf, B. E., K. A. Fahrner, L. Turner, and H. C. Berg. 1998. Control of direction of flagellar rotation in bacterial chemotaxis. *Proc. Natl. Acad. Sci. USA.* 95:201–206.

Shapiro, M. J., and D. E. Koshland, Jr. 1994. Mutagenic studies of the interaction between the aspartate receptor and methyltransferase from *Escherichia coli. J. Biol. Chem.* 269:11054–11059.

Shapiro, M. J., D. Panomitros, and D. E. Koshland, Jr. 1995. Interactions between the methylation sites of *Escherichia coli* aspartate receptor mediated by the methyltransferase. *J. Biol. Chem.* 270:751–755.

Sourjik, V., and H. C. Berg. 2002. Receptor sensitivity in bacterial chemotaxis. *Proc. Natl. Acad. Sci. USA.* 99:123–127.

Spiro, P. A., J. S. Parkinson, and H. G. Othmer. 1997. A model of excitation and adaptation in bacterial chemotaxis. *Proc. Natl. Acad. Sci. USA.* 94:7263–7268.

Yi, T., Y. Huang, M. I. Simon, and J. Doyle. 2000. Robust perfect adaptation in bacterial chemotaxis through integral feedback control. *Proc. Natl. Acad. Sci. USA.* 97:4649–4653.